SCIENCE CHINA
Information Sciences

• RESEARCH PAPER •

July 2025, Vol. 68, Iss. 7, 172202:1–172202:13
https://doi.org/10.1007/s11432-024-4297-4

Composite disturbance filtering and full actuation control for fully observed systems

Chenliang WANG[1,2], Zhihui WANG[1], Wenshuo LI[2], Aiguo WU[3] & Lei GUO[1,2*]

[1]*School of Automation Science and Electrical Engineering, Beihang University, Beijing 100191, China*
[2]*Hangzhou Innovation Institute of Beihang University, Hangzhou 310051, China*
[3]*School of Mechanical Engineering and Automation, Harbin Insitute of Technology, Shenzhen, Shenzhen 518055, China*

Received 25 August 2024/Revised 5 November 2024/Accepted 21 November 2024/Published online 20 March 2025

Abstract Recent several years have witnessed rapid development of the fully actuated system (FAS) approach proposed by Duan in 2020–2021, which considerably facilitates the controller design in comparison with the traditional state-space approach. In this paper, based on high-order system models, the concept of fully observed systems (FOSs) is first proposed as a complementary and dual one of FASs. Then, aiming at a representative class of nonlinear FOSs with multiple heterogenous disturbances, a composite disturbance filtering (CDF) scheme with disturbance compensation and attenuation capabilities is presented. Furthermore, an integrative design of CDF and full actuation control is proposed, which builds bridges among the FAS approach, the composite hierarchical anti-disturbance control, and the CDF. It is proven that the integrative design achieves not only high-precision estimation but also high-precision control and all signals of the resulting closed-loop system are globally uniformly bounded. The effectiveness of the theoretical results is illustrated by numeric simulation and hardware-in-the-loop experiments.

Keywords fully observed systems, fully actuated systems, composite disturbance filtering, anti-disturbance control, integrative design

Citation Wang C L, Wang Z H, Li W S, et al. Composite disturbance filtering and full actuation control for fully observed systems. Sci China Inf Sci, 2025, 68(7): 172202, https://doi.org/10.1007/s11432-024-4297-4

1 Introduction

Practical systems follow certain physical laws such as Newton's laws and Kirchhoff's laws. These physical laws usually model the systems by second-order or high-order differential equations. Motivated by the essential characteristics of practical systems, the fully actuated system (FAS) approach was originally proposed by Duan in 2020–2021 [1–3]. Unlike the traditional state-space approach, which converts second-order and high-order differential equations into first-order ones and may hide some physical meaning, the FAS approach is built upon FAS models and has a clearer physical meaning and simpler design procedure. As a general control methodology, some important issues of the FAS approach were explored in Duan's series of papers, including robust control [4], adaptive control [5], stabilization of generalized chained forms [6, 7], extension to time-delay systems [8, 9], and discrete-time systems [10]. Since its birth, the FAS approach has attracted a great deal of attention in the control community [11–15]. For instance, in [13], it was utilized to solve the tracking control problem of a class of networked systems. In [14, 15], event-triggered adaptive controllers were elegantly designed for strict-feedback nonlinear systems based on the FAS approach. Moreover, recent several years have witnessed its wide applications in spacecraft [16], quadrotors [17], servo systems [18], microgrids [19], and other emerging industries. Readers are referred to [20] for an excellent recent overview of the FAS approach.

Nevertheless, it is noticed that existing results on the FAS approach mainly focused on controller design and analysis, while little attention has been paid to state estimation. As we know, state estimation and controller design are usually dual problems, both of which are fundamental issues in many areas. With the rapid development of the FAS approach, a natural and important question is whether we can give a dual concept of FASs and develop the state estimation counterpart, which motivates the study of this paper. Based on high-order system models, the concept of fully measured systems was proposed in [21],

* Corresponding author (email: lguo@buaa.edu.cn)

where a system is called a fully measured system if there exists a diffeomorphism from its basic state to measurement. However, for general nonlinear systems, fully measured systems may not necessarily be observable, and the state estimation problem remains largely open. Moreover, disturbances, which are inevitable in practical systems, were not considered in [21]. As a result, the applicability of the observers designed in [21] to the case with disturbances needs further investigation.

In the field of state estimation, the most widely used approach is undoubtedly the Kalman filtering, which has optimality for linear systems with Gaussian noises [22, 23]. With respect to non-Gaussian stochastic disturbances, the stochastic distribution filtering was proposed in [24–26]. When it comes to norm-bounded disturbances, the robust technique has been widely incorporated into the observer design [27–29]. Besides, for a class of nonlinear systems with unknown constant parameters, an adaptive observer was designed in [30] to recover state variables with lack of persistency of excitation. A common feature of [22–30] lies in that the system under consideration only suffers from a single type of disturbances. However, as pointed out in [31], practical systems are often faced with multiple types of disturbances that are physically multi-source, mathematically heterogeneous, affecting the systems through isometric channels and coupled with each other, raising an urgent need to develop refined state estimation schemes by making full use of the properties of disturbances.

Stimulated by multiple heterogenous disturbances, the composite hierarchical anti-disturbance control (CHADC) theory has been established and developed since the pioneering work in [32], which flexibly fuses disturbance observers (DOs) and other techniques such as H_∞ control and adaptive control to achieve refined control [33–37]. Inspired by CHADC, the composite disturbance filtering (CDF) was proposed as a novel state estimation methodology for systems with multiple heterogenous disturbances [31, 38, 39], which has a composite "X-DO plus Y-filter" structure. The "X-DO" is designed based on the specific properties of disturbances, while the "Y-filter" covers Kalman filters [40, 41], stochastic distribution filters [42], particle filters [43, 44], H_∞ filters [45], and other advanced filters. Taking the distributed state estimation scheme proposed in [45] for example, it elegantly constructed observers to estimate unknown dynamic disturbances, H_∞ filters to attenuate norm-bounded disturbances, and detection and estimation modules to enhance resilience against deception attacks. Unlike conventional state estimation schemes which lump disturbances into a single one and then either compensate for or attenuate it, CDF simultaneously possesses the capabilities of compensation, attenuation, and utilization of multiple heterogenous disturbances based on refined quantification and effective separation. So far, CDF has been successfully applied to overcome many engineering problems, including initial alignment of inertial navigation systems [38, 39], indoor location of unmanned aerial vehicles [46], and skylight polarization aided integrated attitude determination [31].

In this paper, inspired by the above observation, we investigate CDF and full actuation control for fully observed systems (FOSs). The contribution of this paper includes three aspects. First, based on high-order system models, the concept of FOSs is proposed as a complementary and dual one of FASs. Second, by designing a nonlinear high-gain observer, a CDF scheme is proposed for a class of nonlinear FOSs, which can simultaneously compensate for and attenuate multiple heterogenous disturbances. Third, an integrative design of CDF and full actuation control is presented, which generates a composite refined anti-disturbance controller and builds bridges among the FAS approach, CHADC and CDF. Both high-precision estimation and high-precision control can be achieved by the integrative design in face of multiple heterogenous disturbances, and all signals of the resulting closed-loop system are proven to be globally uniformly bounded.

The remainder of this paper is organized as follows. In Section 2, the concept of FOSs is introduced and some representative FOSs are discussed. In Section 3, a CDF scheme is proposed for a class of nonlinear FOSs with multiple heterogenous disturbances. Section 4 gives the integrative design of CDF and full actuation control, whose effectiveness is illustrated by simulation and experimental results in Section 5. Finally, Section 6 concludes the paper.

2 Fully observed systems

Consider the following system:

$$x^{(m)} = f(x, \dot{x}, \ldots, x^{(m-1)}, u, \dot{u}, \ldots, u^{(m-1)}, t),\ y = c(x), \tag{1}$$

where $x \in \mathbb{R}^{n_x}$ is the basic state, $u \in \mathbb{R}^{n_u}$ and $y \in \mathbb{R}^{n_y}$ are the input and measurement of the system, respectively, and f and c are smooth functions. Let $X = [x^{\mathrm{T}}, \dot{x}^{\mathrm{T}}, \ldots, x^{(m-1)\mathrm{T}}]^{\mathrm{T}} \in \mathbb{R}^{mn_x}$.

Definition 1. The system in (1) is called a fully observed system if there exists a dynamical system in the form of

$$\dot{\varpi} = h(y, \varpi, u, t),\ \hat{X} = \zeta(y, \varpi, u, t), \tag{2}$$

such that $X - \hat{X}$ converges to zero or an arbitrarily small residual set for all $X(0) \in \mathbb{R}^{mn_x}$ and $u \in \mathbb{R}^{n_u}$.

Remark 1. The definition of FOSs can be regarded as a complementary and dual concept of FASs in [3]. A common feature in the definitions of FOSs and FASs lies in that they are both based on high-order system models rather than conventional first-order state-space models. However, they are different concepts. An FOS is not necessarily an FAS and vice versa.

According to Definition 1, we discuss some typical FOSs by starting with the following linear time-invariant system:

$$\dot{z} = Az + bu,\ y = cz, \tag{3}$$

where $z \in \mathbb{R}^{n_z}$, $u \in \mathbb{R}$, and $y \in \mathbb{R}$ denote the states, input, and measurement, respectively, and $A \in \mathbb{R}^{n_z \times n_z}$, $b \in \mathbb{R}^{n_z}$, and $c \in \mathbb{R}^{1 \times n_z}$ are constants. When the system in (3) is observable, one can find a nonsingular linear transformation $\bar{z} = \bar{T}z = [\bar{z}_1, \ldots, \bar{z}_{n_z}]^{\mathrm{T}}$ such that [21]

$$\dot{\bar{z}} = \bar{A}\bar{z} + \bar{b}u,\ y = \bar{c}\bar{z}, \tag{4}$$

where $\bar{c} = [0, \ldots, 0, 1]$ and

$$\bar{A} = \begin{bmatrix} 0 & 0 & \cdots & 0 & -\bar{a}_{n_z} \\ 1 & 0 & \cdots & 0 & -\bar{a}_{n_z-1} \\ 0 & 1 & \cdots & 0 & -\bar{a}_{n_z-2} \\ \vdots & \vdots & \ddots & \vdots & \vdots \\ 0 & 0 & \cdots & 1 & -\bar{a}_1 \end{bmatrix},\ \bar{b} = \begin{bmatrix} \bar{b}_{n_z} \\ \bar{b}_{n_z-1} \\ \vdots \\ \bar{b}_2 \\ \bar{b}_1 \end{bmatrix}. \tag{5}$$

Based on (4) and (5), it can be checked that

$$\begin{aligned} \dot{\bar{z}}_1 &= -\bar{a}_{n_z}\bar{z}_{n_z} + \bar{b}_{n_z}u, \\ \ddot{\bar{z}}_2 &= \dot{\bar{z}}_1 - \bar{a}_{n_z-1}\dot{\bar{z}}_{n_z} + \bar{b}_{n_z-1}\dot{u}, \\ &\vdots \\ \bar{z}_{n_z-1}^{(n_z-1)} &= \bar{z}_{n_z-2}^{(n_z-2)} - \bar{a}_2\bar{z}_{n_z}^{(n_z-2)} + \bar{b}_2u^{(n_z-2)}, \\ \bar{z}_{n_z}^{(n_z)} &= \bar{z}_{n_z-1}^{(n_z-1)} - \bar{a}_1\bar{z}_{n_z}^{(n_z-1)} + \bar{b}_1u^{(n_z-1)}. \end{aligned} \tag{6}$$

By summing the n_z equations in (6), the system in (3) can be rewritten in the form of (1) as

$$\bar{z}_{n_z}^{(n_z)} = -\sum_{i=1}^{n_z} \bar{a}_i\bar{z}_{n_z}^{(n_z-i)} + \sum_{i=1}^{n_z} \bar{b}_iu^{(n_z-i)},\ y = \bar{z}_{n_z}, \tag{7}$$

which implies that the system in (3) is an FOS if it is observable. As a result, with respect to the linear system in (3), if

$$\operatorname{rank}\begin{bmatrix} c \\ cA \\ \vdots \\ cA^{n_z-1} \end{bmatrix} = n_z, \tag{8}$$

then it is an FOS.

As for nonlinear systems, it can be checked that the nonlinear system in the observable canonical form investigated in [21] is fully observed. Besides, the following nonlinear system belongs to FOSs:

$$\dot{z}_1 = z_2 + \varphi_1(y),$$

$$\begin{aligned}\dot{z}_2 &= z_3 + \varphi_2(y),\\ &\vdots\\ \dot{z}_{m-1} &= z_m + \varphi_{m-1}(y),\\ \dot{z}_m &= \eta(y)u + \varphi_m(y),\\ y &= z_1.\end{aligned} \tag{9}$$

Letting $x = z_1$, it can be checked that

$$x^{(i)} = z_{i+1} + \sum_{j=1}^{i} \frac{\mathrm{d}^{i-j}}{\mathrm{d}t^{i-j}}\varphi_j(x),\ i = 1, \ldots, m-1, \tag{10}$$

$$x^{(m)} = \eta(x)u + \sum_{j=1}^{m} \frac{\mathrm{d}^{m-j}}{\mathrm{d}t^{m-j}}\varphi_j(x), \tag{11}$$

which implies that the system in (9) can be rewritten in the form of (1). As mentioned in [47], many practical systems can be described by (9), including single-link robotic manipulators, ship dynamics, and spring-mass-damper systems. Let $E_1 = [1, 0, \ldots, 0]^{\mathrm{T}} \in \mathbb{R}^m$, $E_m = [0, \ldots, 0, 1]^{\mathrm{T}} \in \mathbb{R}^m$, $\varphi(y) = [\varphi_1(y), \ldots, \varphi_m(y)]^{\mathrm{T}} \in \mathbb{R}^m$, and

$$A_0 = \begin{bmatrix} 0_{(m-1)\times 1} & I_{m-1} \\ 0 & 0_{1\times(m-1)} \end{bmatrix} \in \mathbb{R}^{m\times m}, \tag{12}$$

where I_{m-1} denotes the $(m-1)\times(m-1)$ identity matrix. Choose $K = [k_1, \ldots, k_m]^{\mathrm{T}} \in \mathbb{R}^m$ such that the matrix $\Xi := A_0 - KE_1^{\mathrm{T}}$ is Hurwitz. Then, the observer for the system in (9) is constructed as follows:

$$\dot{\hat{z}} = \Xi\hat{z} + \varphi(y) + Ky + E_m\eta(y)u, \tag{13}$$

where $\hat{z} = [\hat{z}_1, \ldots, \hat{z}_m]^{\mathrm{T}} \in \mathbb{R}^m$ is the estimation of $z = [z_1, \ldots, z_m]^{\mathrm{T}} \in \mathbb{R}^m$. From (9) and (13), the estimation error $\tilde{z} := z - \hat{z}$ satisfies

$$\dot{\tilde{z}} = \Xi\tilde{z}, \tag{14}$$

which converges to zero exponentially. Based on $\hat{z}$, the estimations of $\dot{x}, \ldots, x^{(m-1)}$ can be obtained recursively by (10). As a result, the nonlinear system in (9) is an FOS.

Remark 2. Note that the concept of fully measured systems was introduced in [21], where a system is called a fully measured system if there exists a diffeomorphism from its basic state to measurement. For a linear system, if it is equivalent to a high-order fully measured system defined in [21], then it is also fully observed. When it comes to nonlinear systems, the concepts of fully measured systems and FOSs are different, because a fully measured nonlinear system may not necessarily be observable and does not imply the existence of the dynamical system in (2).

3 Composite disturbance filtering

Now, we consider the case that the FOS in (9) suffers from multiple heterogenous disturbances, given by

$$\begin{aligned}\dot{z}_1 &= z_2 + \varphi_1(y),\\ \dot{z}_2 &= z_3 + \varphi_2(y),\\ &\vdots\\ \dot{z}_{m-1} &= z_m + \varphi_{m-1}(y),\\ \dot{z}_m &= \eta(y)u + \varphi_m(y) + d_1(t) + d_2(t),\\ y &= z_1.\end{aligned} \tag{15}$$

In (15), $d_2(t)$ is an unknown bounded disturbance, while $d_1(t)$ represents a disturbance which can be described as [32–37]

$$\dot{\mu} = W\mu,\ d_1 = S\mu, \tag{16}$$

where $\mu \in \mathbb{R}^q$ is unavailable for measurement, $\mu(0)$ is unknown, $W \in \mathbb{R}^{q\times q}$ and $S \in \mathbb{R}^{1\times q}$ are known constants, and the real parts of the eigenvalues of W are nonpositive.

In the presence of the heterogenous disturbances d_1 and d_2, the observer in (13) may become invalid. In what follows, within the framework of CDF, we design a new observer to simultaneously estimate z and the disturbance d_1, while the effect of d_2 will be attenuated. Defining

$$H_1 = \begin{bmatrix} S \\ SW \\ \vdots \\ SW^{q-1} \end{bmatrix}, \tag{17}$$

the following assumption is made.

Assumption 1. H_1 in (17) is a full rank matrix.

Remark 3. The disturbance model in (16) together with Assumption 1 can be widely found in the literature (see [32–37]). As stated in [36, 37], the model in (16) can describe many disturbances such as unknown constant disturbances, sinusoidal disturbances with unknown amplitudes, unknown phases, and known frequencies, unknown exponentially decaying disturbances, and their combinations, while practical examples of such disturbances include dynamic imbalance disturbances in gimbal servo systems, cogging torques in motors, and aerodynamic torques in spacecraft. Assumption 1 ensures the observability of the disturbance described by (16).

Let $Y = [z_1, \ldots, z_m, \mu^{\mathrm{T}}]^{\mathrm{T}} \in \mathbb{R}^{m+q}$, $\bar{\varphi}(y) = [\varphi_1(y), \ldots, \varphi_m(y), 0, \ldots, 0]^{\mathrm{T}} \in \mathbb{R}^{m+q}$, $E_{m+q} = [E_m^{\mathrm{T}}, 0, \ldots, 0]^{\mathrm{T}} \in \mathbb{R}^{m+q}$, $C = [1, 0, \ldots, 0] \in \mathbb{R}^{1\times(m+q)}$, and

$$F = \begin{bmatrix} 0_{(m-1)\times 1} & I_{m-1} & 0_{(m-1)\times q} \\ 0 & 0_{1\times(m-1)} & S \\ 0_{q\times 1} & 0_{q\times(m-1)} & W \end{bmatrix} \in \mathbb{R}^{(m+q)\times(m+q)}. \tag{18}$$

Then, it follows from (15) and (16) that

$$\dot{Y} = FY + \bar{\varphi}(y) + E_{m+q}[\eta(y)u + d_2(t)],\ y = CY. \tag{19}$$

Let

$$H_2 = \begin{bmatrix} C \\ CF \\ \vdots \\ CF^{m+q-1} \end{bmatrix}. \tag{20}$$

Lemma 1. Under Assumption 1, H_2 in (20) is a full rank matrix.

Proof. By calculation, it follows from (17), (18), and (20) that

$$H_2 = \begin{bmatrix} I_m & 0_{m\times q} \\ 0_{q\times m} & H_1 \end{bmatrix}. \tag{21}$$

Noting from Assumption 1 that $\mathrm{rank}(H_1) = q$, we have $\mathrm{rank}(H_2) = m + q$. Hence, H_2 is a full rank matrix, which completes the proof.

Since H_2 is a full rank matrix, the eigenvalues of the matrix $(F - LC)$ can be arbitrarily assigned by appropriately choosing $L \in \mathbb{R}^{1\times(m+q)}$. Introducing a constant $\alpha \geqslant 1$ as a design parameter, we choose L such that all eigenvalues of $(F - LC)$ are equal to $-\alpha$. This choice ensures that the matrix $(F - LC + \frac{3}{4}\alpha I_{m+q})$ is Hurwitz. Furthermore, there exists a symmetric positive definite matrix $P \in \mathbb{R}^{(m+q)\times(m+q)}$ such that

$$\left(F - LC + \frac{3}{4}\alpha I_{m+q}\right)^{\mathrm{T}} P + P\left(F - LC + \frac{3}{4}\alpha I_{m+q}\right) = -I_{m+q}. \tag{22}$$

Now, the observer in the presence of multiple heterogenous disturbances is designed as

$$\dot{\hat{Y}} = (F - LC)\hat{Y} + \bar{\phi}(y) + Ly + E_{m+q}\eta(y)u, \tag{23}$$

where $\hat{Y} = [\hat{z}_1, \ldots, \hat{z}_m, \hat{\mu}^{\mathrm{T}}]^{\mathrm{T}} \in \mathbb{R}^{m+q}$ is the estimation of Y. The estimation of d_1 is given by $\hat{d}_1 = S\hat{\mu}$.

Theorem 1. Consider the nonlinear system in (15) under Assumption 1. The observer in (23) can steer the estimation error $\tilde{Y} = Y - \hat{Y}$ into a residual set which can be made arbitrarily small by increasing the design parameter α. Particularly, if $\lim_{t\to+\infty} d_2(t) = 0$, then $\lim_{t\to+\infty} \tilde{Y}(t) = 0$.

Proof. Using (19) and (23), it can be proven that

$$\dot{\tilde{Y}} = (F - LC)\tilde{Y} + E_{m+q}d_2(t). \tag{24}$$

With the matrix P in (22), define $V_1 = \tilde{Y}^{\mathrm{T}}P\tilde{Y}$, whose derivative along the solution of (24) yields

$$\dot{V}_1 = -\tilde{Y}^{\mathrm{T}}\tilde{Y} - \frac{3}{2}\alpha\tilde{Y}^{\mathrm{T}}P\tilde{Y} + 2\tilde{Y}^{\mathrm{T}}PE_{m+q}d_2(t). \tag{25}$$

It follows from Young's inequality that

$$2\tilde{Y}^{\mathrm{T}}PE_{m+q}d_2(t) \leqslant \frac{1}{2}\tilde{Y}^{\mathrm{T}}P\tilde{Y} + 2d_2^2(t)E_{m+q}^{\mathrm{T}}PE_{m+q} \leqslant \frac{1}{2}\tilde{Y}^{\mathrm{T}}P\tilde{Y} + \theta, \tag{26}$$

where $\theta := 2p_{mm}\sup_{t\geqslant 0} d_2^2(t)$ with p_{mm} the (m,m)th element of P. Substituting (26) into (25) and noting $\alpha \geqslant 1$, we have

$$\dot{V}_1 \leqslant -\alpha V_1 + \theta. \tag{27}$$

Solving (27) gives

$$0 \leqslant V_1(t) \leqslant \frac{\theta}{\alpha} + \left[V_1(0) - \frac{\theta}{\alpha}\right]\mathrm{e}^{-\alpha t},\ \forall t \geqslant 0. \tag{28}$$

Therefore,

$$\lim_{t\to+\infty} ||\tilde{Y}(t)|| \leqslant \lim_{t\to+\infty} \sqrt{\frac{V_1(t)}{\lambda_{\max}(P)}} \leqslant \sqrt{\frac{\theta}{\alpha\lambda_{\max}(P)}}. \tag{29}$$

It is clear from (29) that the estimation error $\tilde{Y}(t)$ converges to a residual set that can be made arbitrarily small by increasing the design parameter α. Particularly, by (24), we know $\lim_{t\to+\infty} \tilde{Y}(t) = 0$ if $\lim_{t\to+\infty} d_2(t) = 0$, which completes the proof.

Remark 4. The core of our CDF scheme is the nonlinear observer designed in (23). The observer has a high-gain feature because the distance between the imaginary axis and the eigenvalues of the matrix $(F - LC)$, represented by α, is used as a design parameter no less than 1. This parameter plays a key role in guaranteeing the estimation precision in the presence of d_2. If α is a fixed constant, then the estimation error $\tilde{Y}$ cannot be made arbitrarily small, as can be seen from (29). The advantage of the observer mainly lies in that it can simultaneously compensate for and attenuate multiple heterogeneous disturbances. It simultaneously estimates the system states and the disturbance d_1 by fully using model information and compensates for d_1 via its estimation. Meanwhile, it can attenuate the effect of the unknown bounded disturbance d_2 by adjusting α. Note that the observability of the nonlinear system in (19) is not obtained from a rank criterion. It is obtained after we construct the observer in (23) and prove the convergence of the estimation error in Theorem 1.

4 Integrative design of CDF and full actuation control

Consider the single-link robotic manipulator shown in Figure 1, whose dynamics is given by [48]

$$\ddot{y} + \frac{\sigma}{a}\dot{y} + \frac{Mgl}{a}\sin(y) = \frac{1}{a}u + d_1(t) + d_2(t), \tag{30}$$

where y is the link angle, u is the control torque, a, σ, M, g, and l are the rotational inertia, damping coefficient, link mass, gravitational acceleration, and distance from the joint axis to the link center of mass,

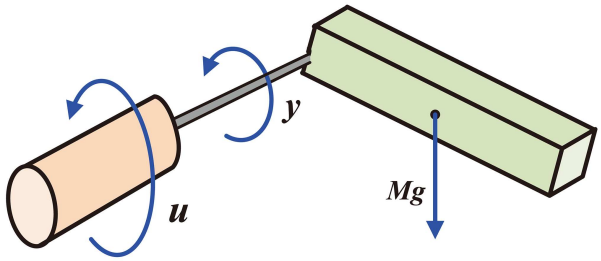

Figure 1 (Color online) Single-link robotic manipulator.

respectively, $d_1(t)$ is a disturbance described by (16), and $d_2(t)$ is an unknown bounded disturbance. It is assumed that the parameters a, σ, M, g, and l are known and the link angular velocity $\dot{y}$ is unmeasured. Letting

$$z_1 = y,\ z_2 = \dot{y} + \frac{\sigma}{a}y, \tag{31}$$

we have

$$\dot{z}_1 = z_2 - \frac{\sigma}{a}y,\ \dot{z}_2 = \frac{1}{a}u - \frac{Mgl}{a}\sin(y) + d_1(t) + d_2(t). \tag{32}$$

Obviously, the single-link robotic manipulator is a special case of (15) and thus is an FOS. Meanwhile, according to the definition of [3], the single-link robotic manipulator is also an FAS. In what follows, we shall design a refined anti-disturbance controller for the single-link robotic manipulator based on the CDF scheme in Section 3 and the FAS approach.

The control objective is to design the control input u such that all signals of the resulting closed-loop system are bounded and the link angle y tracks a desired trajectory y_d, where y_d, $\dot{y}_d$, and $\ddot{y}_d$ are bounded. The observer for (32) can be readily obtained based on the results in Section 3, given by

$$\dot{\hat{Y}} = (F - LC)\hat{Y} + \bar{\phi}(y) + Ly + Bu, \tag{33}$$

where $\hat{Y} = [\hat{z}_1, \hat{z}_2, \hat{\mu}^{\mathrm{T}}]^{\mathrm{T}} \in \mathbb{R}^{2+q}$ is the estimation of $Y = [z_1, z_2, \mu^{\mathrm{T}}]^{\mathrm{T}} \in \mathbb{R}^{2+q}$, $\bar{\varphi}(y) = [-\frac{\sigma}{a}y, -\frac{Mgl}{a}\sin(y), 0, \ldots, 0]^{\mathrm{T}} \in \mathbb{R}^{2+q}$, $B = [0, \frac{1}{a}, 0, \ldots, 0]^{\mathrm{T}} \in \mathbb{R}^{2+q}$, and $C = [1, 0, \ldots, 0] \in \mathbb{R}^{1\times(2+q)}$. The estimation of the link angular velocity $\dot{y}$ and the disturbance d_1 are given by $\hat{\dot{y}} = \hat{z}_2 - \frac{\sigma}{a}y$ and $\hat{d}_1 = S\hat{\mu}$, respectively. Under Assumption 1, the conclusion in Theorem 1 is valid for (32) and (33).

Define the tracking error

$$\beta = y - y_d. \tag{34}$$

In view of (30), the dynamics of β can be expressed in form of second-order FASs as

$$\ddot{\beta} = \frac{1}{a}u - \frac{\sigma}{a}\dot{y} - \frac{Mgl}{a}\sin(y) - \dot{y}_d + d_1(t) + d_2(t). \tag{35}$$

Introducing a constant $r \geqslant 1$ as a design parameter, Eq. (35) can be rewritten as

$$\ddot{\beta} = -r^2\beta - 2r\dot{\beta} + \frac{1}{a}u + \tau + \left(2r - \frac{\sigma}{a}\right)z_2 + d_1(t) + d_2(t), \tag{36}$$

where

$$\tau = r^2\beta - \frac{Mgl}{a}\sin(y) - \dot{y}_d - 2r\dot{y}_d - \frac{\sigma}{a}\left(2r - \frac{\sigma}{a}\right)y. \tag{37}$$

Now, the control law is designed as

$$u = -a\left[\tau + \left(2r - \frac{\sigma}{a}\right)\hat{z}_2 + \hat{d}_1\right], \tag{38}$$

which results in

$$\ddot{\beta} = -r^2\beta - 2r\dot{\beta} + \left(2r - \frac{\sigma}{a}\right)\tilde{z}_2 + \tilde{d}_1(t) + d_2(t), \tag{39}$$

with $\tilde{z}_2 = z_2 - \hat{z}_2$ and $\tilde{d}_1 = d_1 - \hat{d}_1 = S\tilde{\mu}$.

Theorem 2. Consider the closed-loop system composed of the single-link robotic manipulator in (30), the observer in (33), and the control law in (38). Suppose that Assumption 1 holds. Then, all signals of the closed-loop system are globally uniformly bounded, and the tracking error β converges to a residual set which can be made arbitrarily small by properly choosing the design parameters. Particularly, if $\lim_{t\to+\infty} d_2(t)=0$, then $\lim_{t\to+\infty}\beta(t)=0$.

Proof. Define $\phi_1=[\beta,\dot{\beta}]^{\mathrm{T}}$, and

$$\Lambda_1=\begin{bmatrix}0 & 1\\ -r^2 & -2r\end{bmatrix},\ \Lambda_2=\begin{bmatrix}0 & 1\\ -1 & -2\end{bmatrix}. \tag{40}$$

It follows from (39) that

$$\dot{\phi}_1=\Lambda_1\phi_1+\begin{bmatrix}0\\ (2r-\frac{\sigma}{a})\tilde{z}_2+\tilde{d}_1(t)+d_2(t)\end{bmatrix}. \tag{41}$$

Letting $\phi_2=\Gamma\phi_1$ with $\Gamma=\mathrm{diag}\{r,1\}$, we have $\Gamma\Lambda_1\Gamma^{-1}=r\Lambda_2$ and

$$\dot{\phi}_2=r\Lambda_2\phi_2+\begin{bmatrix}0\\ (2r-\frac{\sigma}{a})\tilde{z}_2+\tilde{d}_1(t)+d_2(t)\end{bmatrix}. \tag{42}$$

Let $V_2=\phi_2^{\mathrm{T}}Q\phi_2$, where the symmetric positive definite matrix $Q\in\mathbb{R}^{2\times2}$ is the solution of $\Lambda_2^{\mathrm{T}}Q+Q\Lambda_2=-I_2$. In view of (42), differentiating V_2 gives

$$\begin{aligned}\dot{V}_2 &= -r\phi_2^{\mathrm{T}}\phi_2+2\phi_2^{\mathrm{T}}Q\begin{bmatrix}0\\ \left(2r-\frac{\sigma}{a}\right)\tilde{z}_2+\tilde{d}_1(t)+d_2(t)\end{bmatrix}\\ &\leqslant -\frac{r}{2}\phi_2^{\mathrm{T}}\phi_2+\frac{2||Q||^2}{r}\left[\left(2r-\frac{\sigma}{a}\right)\tilde{z}_2+\tilde{d}_1(t)+d_2(t)\right]^2\\ &\leqslant -\frac{r}{2\lambda_{\max}(Q)}V_2+2||Q||^2\left[\left(2-\frac{\sigma}{ar}\right)\tilde{z}_2+\frac{\tilde{d}_1(t)+d_2(t)}{r}\right]^2.\end{aligned} \tag{43}$$

By Theorem 1, $\tilde{z}_2$ and $\tilde{d}_1(t)$ are bounded. With this fact in mind and noting $r\geqslant1$, we know there exists a positive constant D independent of r such that

$$2||Q||^2\left[\left(2-\frac{\sigma}{ar}\right)\tilde{z}_2+\frac{\tilde{d}_1(t)+d_2(t)}{r}\right]^2\leqslant D,\ \forall t\geqslant0. \tag{44}$$

Substituting (44) into (43) gives

$$\dot{V}_2\leqslant-\frac{r}{2\lambda_{\max}(Q)}V_2+D, \tag{45}$$

which implies that

$$0\leqslant V_2(t)\leqslant\frac{2D\lambda_{\max}(Q)}{r}+\left[V_2(0)-\frac{2D\lambda_{\max}(Q)}{r}\right]\mathrm{e}^{\frac{-rt}{2\lambda_{\max}(Q)}},\ \forall t\geqslant0. \tag{46}$$

It is clear from (46) that V_2, β, and $\dot{\beta}$ are bounded. Then, taking Theorem 1 into consideration, it can be concluded that all signals of the closed-loop system are globally uniformly bounded. Moreover, we know from (46) that

$$\lim_{t\to+\infty}|\beta(t)|\leqslant\frac{1}{r}\lim_{t\to+\infty}||\phi_2(t)||\leqslant\frac{1}{r}\lim_{t\to+\infty}\sqrt{\frac{V_2(t)}{\lambda_{\min}(Q)}}\leqslant\sqrt{\frac{2D\lambda_{\max}(Q)}{r^3\lambda_{\min}(Q)}}. \tag{47}$$

Thus, the tracking error β converges to a residual set which can be made arbitrarily small by increasing the design parameter r. On the other hand, in the case of $\lim_{t\to+\infty}d_2(t)=0$, it follows from Theorem 1 that $\lim_{t\to+\infty}2||Q||^2\big[(2-\frac{\sigma}{ar})\tilde{z}_2(t)+\frac{\tilde{d}_1(t)+d_2(t)}{r}\big]^2=0$, which together with (43) gives $\lim_{t\to+\infty}\beta(t)=0$. This completes the proof.

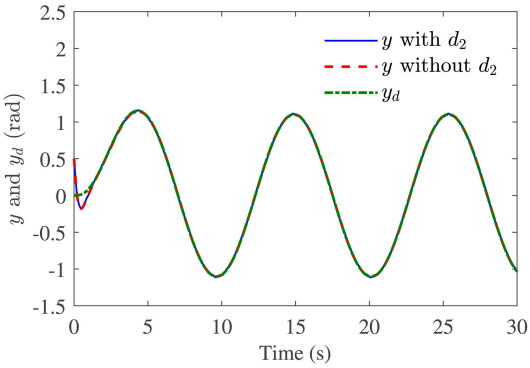

Figure 2 (Color online) Link angle y and desired trajectory y_d in simulation.

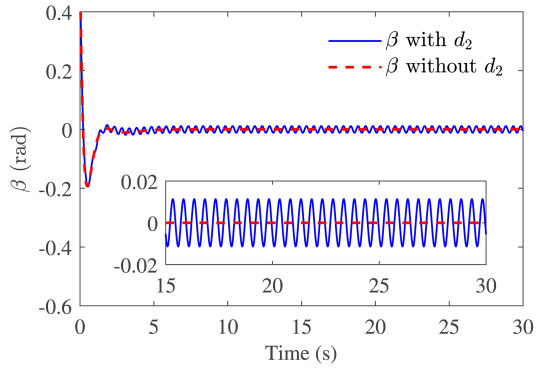

Figure 3 (Color online) Tracking error β in simulation.

Remark 5. The above integrative design covers the observer design based on CDF and the controller design, where the controller fuses the features of full actuation control and CHADC. Therefore, the integrative design builds bridges among the FAS approach, CHADC, and CDF. Similar to the observer, the controller compensates for the disturbance d_1 based on its estimation and attenuates the effect of the disturbance d_2 by increasing the design parameter r. As can be seen from Theorems 1 and 2, the integrative design achieves not only high-precision estimation but also high-precision control and successfully ensures global stability of the closed-loop system in face of multiple heterogenous disturbances. Besides, it can be extended to the general case of the high-order system in (15) with the aid of the backstepping technique [4].

5 Simulation and experimental results

In this section, simulation and experimental results on the robotic manipulator in (30) are presented to illustrate the effectiveness of the integrative design. In the simulation and experiments, the parameters and the initial conditions of the robotic manipulator are set as $a = 0.03$ kg·m^2, $\sigma = 0.12$ N·m·s/rad, $M = 0.1$ kg, $g = 9.8$ m/s^2, $l = 0.15$ m, $y(0) = 0.5$ rad, and $\dot{y}(0) = -0.2$ rad/s. The desired trajectory y_d is generated by $\ddot{y}_d + 2\dot{y}_d + y_d = 1.5\sin(0.6t)$ with $y_d(0) = 0$ rad and $\dot{y}_d(0) = 0$ rad/s. The disturbance $d_2(t)$ is completely unknown but bounded, which is set as a triangular wave with frequency 2 Hz and magnitude 2. The disturbance $d_1(t)$ is set as a sinusoidal wave with unknown amplitude, unknown phase, and known frequency, given by $d_1(t) = \varepsilon\sin(t + \varrho)$ with ε and ϱ unknown constants. Note that $d_1(t)$ can be described by (16) with $\mu(0) = [-\varepsilon\cos(\varrho), \varepsilon\sin(\varrho)]^{\mathrm{T}}$ and

$$S = [0, 1],\ W = \begin{bmatrix} 0 & 1 \\ -1 & 0 \end{bmatrix}. \tag{48}$$

In the simulation and experiments, we set $\varepsilon = \sqrt{2}$ and $\varrho = -\frac{3}{4}\pi$. It can be checked that the matrices in (48) satisfy Assumption 1.

5.1 Simulation results

In the simulation, the sampling period is set as 0.0001 s, the design parameters α and r are chosen as $\alpha = 2$ and $r = 12$, where the vector L corresponding to $\alpha = 2$ is calculated as $L = [8, 23, 7, 24]^{\mathrm{T}}$. Both the case with d_2 and the case without d_2 are considered, and the simulation results are shown in Figures 2–7. As can be seen from Figures 2–7, for the case with d_2, our controller makes the link angle y well track the desired trajectory y_d with the tracking error β converging to a small residual set, and our observer can simultaneously estimate the link angular velocity $\dot{y}$ and the disturbance d_1 with the estimation errors $\delta := \dot{y} - \hat{\dot{y}}$ and $\tilde{d}_1$ converging to small residual sets. As for the case without d_2, it is observed that the tracking error and the estimation errors converge to zero asymptotically. The simulation results are consistent with the conclusion in Theorems 1 and 2.

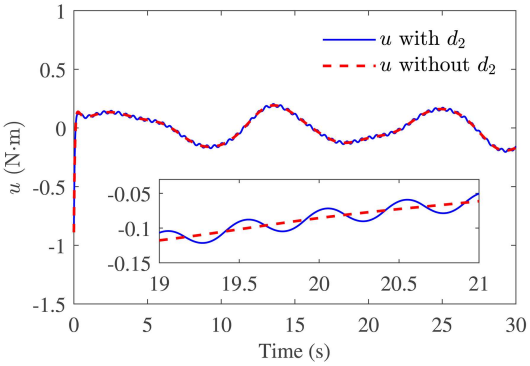

Figure 4 (Color online) Control torque u in simulation.

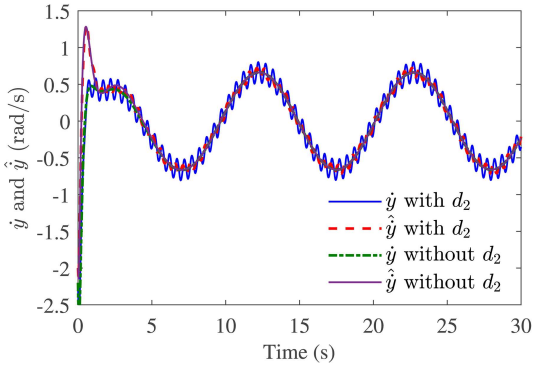

Figure 5 (Color online) Velocity $\dot{y}$ and its estimation $\hat{\dot{y}}$ in simulation.

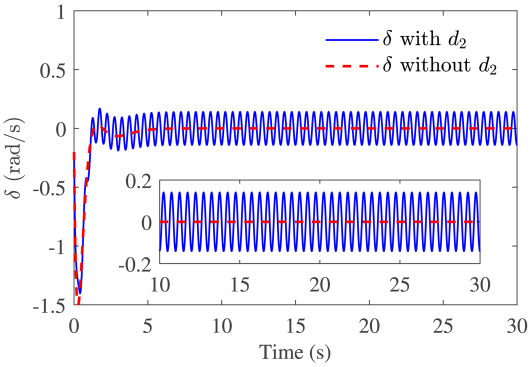

Figure 6 (Color online) Velocity estimation error δ in simulation.

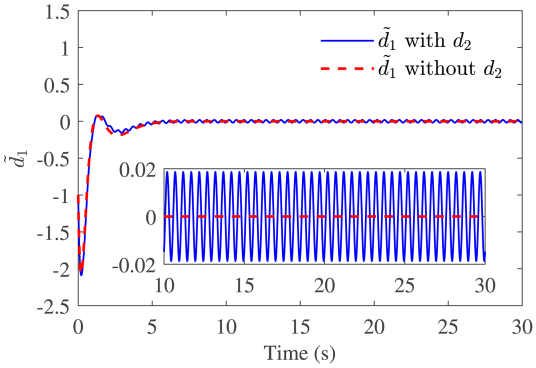

Figure 7 (Color online) Disturbance estimation error $\tilde{d}_1$ in simulation.

5.2 Experimental results

The experimental platform with hardware in the loop is shown in Figure 8, which is mainly composed of a host computer, a real-time simulator, a driving motor, a load motor, sensors, servo drives, and a power supply. The host computer communicates with the real-time simulator through interoperability standard open platform communications and application programming interface. The real-time simulator calculates the control signal and communicates with the two motors. The control torque u and the gravity moment $Mgl\sin(y)$ in (30) are generated by the driving motor and the load motor, respectively, both of which can be measured by torque sensors. The rest parts in (30) are constructed in the host computer and the real-time simulator numerically, where the disturbance $d_2(t)$ is a triangular wave with frequency 2 Hz and magnitude 2. The sampling period T^* of the experimental platform is $T^* = 0.0001$ s.

To test the effects of the design parameters α and r, two cases are considered in the experiments. In the first case, we choose $\alpha = 2$ and $r = 12$, while in the second case, we choose $\alpha = 1.5$ and $r = 10$. The values of L corresponding to $\alpha = 2$ and $\alpha = 1.5$ are $L = [8, 23, 7, 24]^{\mathrm{T}}$ and $L = [6, 12.5, 7.4375, 7.5]^{\mathrm{T}}$, respectively. All other conditions of the two cases are the same, and the experimental results are shown in Figures 9–14. For a quantitative comparison, we introduce the root mean squared error (RMSE) indexes $\Delta_\beta = \sqrt{\frac{1}{N}\sum_{i=1}^{N}\beta_i^2}$, $\Delta_\delta = \sqrt{\frac{1}{N}\sum_{i=1}^{N}\delta_i^2}$, and $\Delta_d = \sqrt{\frac{1}{N}\sum_{i=1}^{N}\tilde{d}_{1,i}^2}$ and the energy consumption index $G_u = T^*\sum_{i=1}^{N}u_i^2$, where $N = 3\times 10^5$ is the number of sampling points, and β_i, δ_i, $\tilde{d}_{1,i}$, and u_i represent the values of β, δ, $\tilde{d}_1$, and u at the ith sampling instant, respectively. Table 1 gives the values of these indexes in the two cases. Compared with those in the second case, the RMSE indexes Δ_β, Δ_δ, and Δ_d in the first case are reduced by 39.29%, 32.57%, and 33.88%, respectively, while the energy consumption index G_u in the first case is slightly increased by 4.26%. The experimental results indicate that increasing α and r can reduce the tracking error and the estimation errors, but a tradeoff should be made among the tracking performance, the estimation performance, and the control effort.

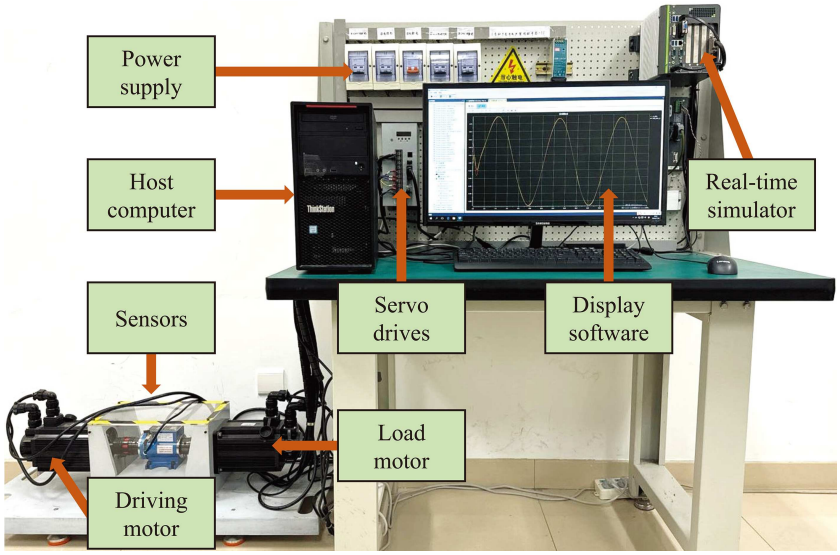

Figure 8 (Color online) Experiment platform.

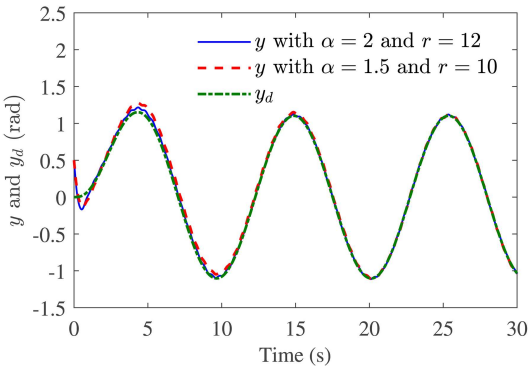

Figure 9 (Color online) Link angle y and desired trajectory y_d in experiments.

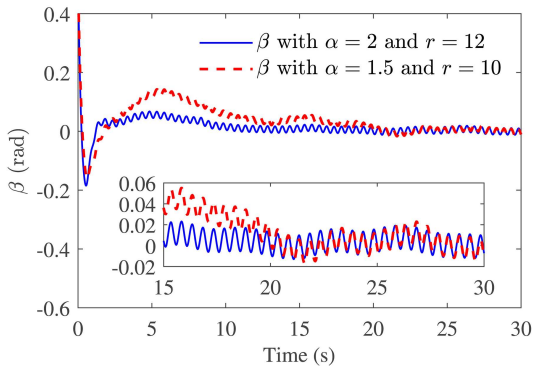

Figure 10 (Color online) Tracking error β in experiments.

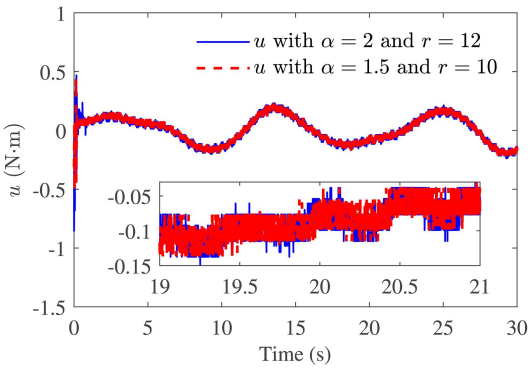

Figure 11 (Color online) Control torque u in experiments.

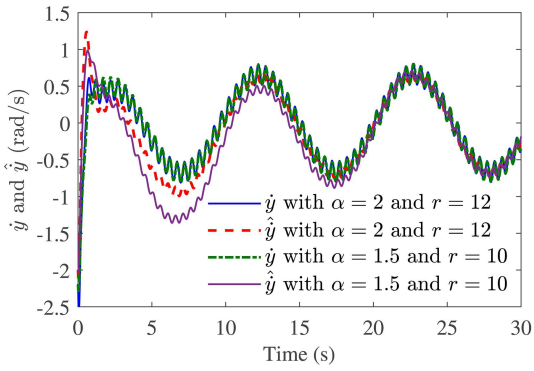

Figure 12 (Color online) Velocity $\dot{y}$ and its estimation $\hat{\dot{y}}$ in experiments.

Table 1 Indexes with different design parameters in experiments.

Values of α and r	Δ_β (rad)	Δ_δ (rad/s)	Δ_d	G_u
$\alpha = 2$, $r = 12$	0.0394	0.2362	0.3444	0.3814
$\alpha = 1.5$, $r = 10$	0.0649	0.3503	0.5209	0.3658

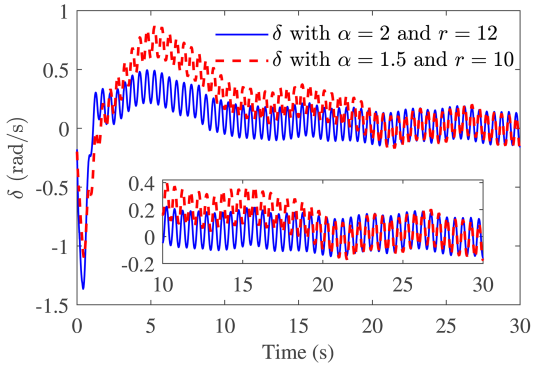

Figure 13 (Color online) Velocity estimation error δ in experiments.

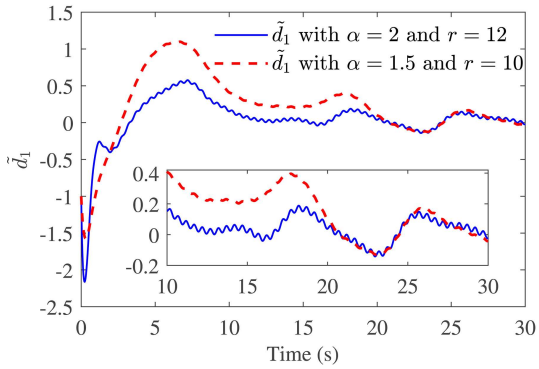

Figure 14 (Color online) Disturbance estimation error $\tilde{d}_1$ in experiments.

6 Conclusion

In this paper, the concept of FOSs has been proposed, and some representative FOSs have been discussed. Taking a class of nonlinear FOSs for example, a CDF strategy has been developed, which can simultaneously compensate for and attenuate multiple heterogenous disturbances. Subsequently, an integrative design framework has been presented to build bridges among the FAS approach, CHADC, and CDF. The integrative design achieves not only high-precision estimation but also high-precision control and possesses enhanced anti-disturbance capability. We have proven that the resulting closed-loop system is globally stable, and the theoretical results have been validated by numeric simulation and hardware-in-the-loop experiments. Nevertheless, our CDF strategy and integrative design require system parameters to be known. Future investigation should include the disposal of parametric uncertainties and the extension to more general high-order nonlinear systems.

Acknowledgements This work was supported by National Natural Science Foundation of China (Grant Nos. 62422302, 62373033, 62122007).

References

1 Duan G. High-order system approaches: I. Fully-actuated systems and parametric designs (in Chinese). Acta Autom Sin, 2020, 46: 1333–1345
2 Duan G. High-order system approaches: II. Controllability and full-actuation (in Chinese). Acta Autom Sin, 2020, 46: 1571–1581
3 Duan G R. High-order fully actuated system approaches: Part I. Models and basic procedure. Int J Syst Sci, 2021, 52: 422–435
4 Duan G R. High-order fully actuated system approaches: Part III. Robust control and high-order backstepping. Int J Syst Sci, 2021, 52: 952–971
5 Duan G R. High-order fully actuated system approaches: Part IV. Adaptive control and high-order backstepping. Int J Syst Sci, 2021, 52: 972–989
6 Duan G R. A FAS approach for stabilization of generalized chained forms: part 1. Discontinuous control laws. Sci China Inf Sci, 2024, 67: 122201
7 Duan G R. A FAS approach for stabilization of generalized chained forms: part 2. Continuous control laws. Sci China Inf Sci, 2024, 67: 132201
8 Duan G R. Fully actuated system approaches for continuous-time delay systems: part 1. Systems with state delays only. Sci China Inf Sci, 2023, 66: 112201
9 Duan G R. Fully actuated system approaches for continuous-time delay systems: part 2. Systems with input delays. Sci China Inf Sci, 2023, 66: 122201
10 Duan G R. Discrete-time delay systems: part 1. Global fully actuated case. Sci China Inf Sci, 2022, 65: 182201
11 Yan F, Zhang M, Gu G. Adaptive estimation and control for uncertain nonlinear systems and full actuation control. Sci China Inf Sci, 2023, 66: 212204
12 Cai M, He X, Zhou D. An active fault tolerance framework for uncertain nonlinear high-order fully-actuated systems. Automatica, 2023, 152: 110969
13 Zhang D W, Liu G P. Predictive sliding-mode control of networked high-order fully actuated systems under random deception attacks. Sci China Inf Sci, 2023, 66: 190204
14 Wang Y, Duan G R, Li P. Event-based neural networks adaptive control of nonlinear systems: a fully actuated system approach. IEEE Trans Circuits Syst I, 2024, 71: 4211–4221
15 Wang Y, Duan G R, Li P. Event-triggered adaptive control of uncertain strict-feedback nonlinear systems using fully actuated system approach. IEEE Trans Cybern, 2024, 54: 6371–6383
16 Zhao T Y, Duan G R. Fully actuated system approach to attitude control of flexible spacecraft with nonlinear time-varying inertia. Sci China Inf Sci, 2022, 65: 212201
17 Wang X, Duan G R. Comprehensive reconstructions and predictive control for quadrotor UAV information gathering tracking missions based on fully actuated system approaches. ISA Trans, 2024, 147: 540–553
18 Li P, Duan G R. High-order fully actuated control approach for servo systems based on dynamical compensator and extended state observer. IEEE ASME Trans Mechatron, 2024, 29: 3717–3726
19 Yu Y, Liu G P, Huang Y, et al. Coordinated predictive secondary control for DC microgrids based on high-order fully actuated system approaches. IEEE Trans Smart Grid, 2024, 15: 19–33

20 Duan G R. Fully actuated system approach for control: an overview. IEEE Trans Cybern, 2024, 54: 7285–7306
21 Duan G R. High-order system approaches: observability and observer design (in Chinese). Acta Autom Sin, 2020, 46: 1885–1895
22 Kalman R E. A new approach to linear filtering and prediction problems. J Basic Eng, 1960, 82: 35–45
23 Kalman R E, Bucy R S. New results in linear filtering and prediction theory. J Basic Eng, 1961, 83: 95–108
24 Guo L, Wang H. Fault detection and diagnosis for general stochastic systems using B-spline expansions and nonlinear filters. IEEE Trans Circuits Syst I, 2005, 52: 1644–1652
25 Guo L, Yin L P, Wang H, et al. Entropy optimization filtering for fault isolation of nonlinear non-Gaussian stochastic systems. IEEE Trans Automat Contr, 2009, 54: 804–810
26 Guo L, Wang H. Stochastic Distribution Control System Design: A Convex Optimization Approach. London: Springer-Verlag, 2010
27 Wang Z D, Yang F W, Ho D W C, et al. Robust H_∞ filtering for stochastic time-delay systems with missing measurements. IEEE Trans Signal Process, 2006, 54: 2579–2587
28 Astolfi D, Marconi L, Praly L, et al. Low-power peaking-free high-gain observers. Automatica, 2018, 98: 169–179
29 Guo X, Wang C, Dong Z, et al. Secure state estimation for nonlinear systems under sparse attacks with application to robotic manipulators. IEEE Trans Ind Electron, 2023, 70: 8408–8415
30 Tomei P, Marino R. An enhanced feedback adaptive observer for nonlinear systems with lack of persistency of excitation. IEEE Trans Automat Contr, 2023, 68: 5067–5072
31 Guo L, Li W, Zhu Y, et al. Composite disturbance filtering: a novel state estimation scheme for systems with multisource, heterogeneous, and isomeric disturbances. IEEE Open J Ind Electron Soc, 2023, 4: 387–400
32 Guo L, Chen W H. Disturbance attenuation and rejection for systems with nonlinearity via DOBC approach. Int J Robust Nonlinear Control, 2005, 15: 109–125
33 Wei X, Guo L. Composite disturbance-observer-based control and H_∞ control for complex continuous models. Int J Robust Nonlinear Control, 2010, 20: 106–118
34 Guo L, Cao S. Anti-Disturbance Control for Systems With Multiple Disturbances. Boca Raton: CRC Press, 2013
35 Zhu Y K, Guo L, Yu X, et al. An enhanced anti-disturbance control law for systems with multiple disturbances. Sci China Inf Sci, 2020, 63: 209206
36 Wang C, Guo L, Wen C, et al. Attitude coordination control for spacecraft with disturbances and event-triggered communication. IEEE Trans Aerosp Electron Syst, 2021, 57: 586–596
37 Wang C, Guo L, Wen C, et al. Adaptive anti-disturbance control for a class of uncertain nonlinear systems with composite disturbances. IEEE Trans Cybern, 2024, 54: 4241–4254
38 Guo L, Cao S, Qi C, et al. Initial alignment for nonlinear inertial navigation systems with multiple disturbances based on enhanced anti-disturbance filtering. Int J Control, 2012, 85: 491–501
39 Cao S, Guo L. Multi-objective robust initial alignment algorithm for inertial navigation system with multiple disturbances. Aerospace Sci Tech, 2012, 21: 1–6
40 Du T, Guo L. Unbiased information filtering for systems with missing measurement based on disturbance estimation. J Franklin Inst, 2016, 353: 936–954
41 Du T, Guo L, Yang J. A fast initial alignment for SINS based on disturbance observer and Kalman filter. Trans Inst Meas Control, 2016, 38: 1261–1269
42 Yi Y, Zheng W X, Sun C, et al. DOB fuzzy controller design for non-Gaussian stochastic distribution systems using two-step fuzzy identification. IEEE Trans Fuzzy Syst, 2016, 24: 401–418
43 Li W, Guo L. Robust particle filtering with time-varying model uncertainty and inaccurate noise covariance matrix. IEEE Trans Syst Man Cybern Syst, 2021, 51: 7099–7108
44 Li W, Liu X, Guo L. Robust particle filtering with state transition uncertainties: a student's t disturbance observer-based approach. IEEE Trans Instrum Meas, 2021, 70: 1–13
45 Guo X, Cao S, Ding Z. Enhanced distributed state estimation with resilience to multiple disturbances and false data injection attacks. Int J Robust Nonlinear Control, 2022, 32: 1075–1092
46 Jia J, Guo K, Li W, et al. Composite filtering for UWB-based localization of quadrotor UAV with skewed measurements and uncertain dynamics. IEEE Trans Instrum Meas, 2022, 71: 1–13
47 Wang C, Guo L, Wen C, et al. Adaptive neural network control for a class of nonlinear systems with unknown control direction. IEEE Trans Syst Man Cybern Syst, 2020, 50: 4708–4718
48 Wang C, Wen C, Guo L. Adaptive consensus control for nonlinear multiagent systems with unknown control directions and time-varying actuator faults. IEEE Trans Automat Contr, 2021, 66: 4222–4229